Halloysite nanotubes and thymol as photo protectors of biobased Polyamide 11

Giuliana Gorrasi[1], Valeria Bugatti[1], Martina Ussia [2], Raniero Mendichi[3], Daniela Zampino[4], Concetto Puglisi[4] and Sabrina Carola Carroccio[4, 5*]

[1]Dipartimento di Ingegneria Industriale, Università degli studi di Salerno, Via Giovanni Paolo II, 132, 84084 Fisciano (SA), Italy.

[3] Consiglio Nazionale delle Ricerche, CNR-ISMAC, Via A. Corti 12, 20133 Milano, Italy

[4]Consiglio Nazionale delle Ricerche, CNR-IPCB s.s Catania, Via P. Gaifami 18, 95126, Italy

[5]Consiglio Nazionale delle Ricerche, CNR-IMM s.s Catania (Università), Via P. Gaifami 18, 95126, Italy

Abstract

The formulation of cost-effectiveness sustainable materials is extensively growing and becoming an attractive approach for both industrial and academic fields. In this context, the bio-based aliphatic polyamide 11 (PA11) has acquired significant interest as environmentally friendly thermoplastic option. In addition, its formulation with selected natural antioxidant and/or reinforced compounds through green processing methods, might improve physical and mechanical properties without sacrificing the intrinsic bio-based nature of the matrix. In this work, we have investigated and compared the photo-oxidative degradation processes occurring on PA11 composites based on thymol and halloysite nanotubes prepared by using ball-milling method. In particular, halloysite nanotubes were used as green nano-container of a natural antioxidant molecule, and reinforced nano-filler as well. Molecular and structural information of photo-exposed samples were obtained by using size exclusion chromatography (SEC) and matrix-assisted laser desorption ionization time-of-flight mass spectrometry (MALDI-TOF MS). Thermal and mechanical properties were also tested as well as thymol release. Data collected confirmed that PA11 filled with HNTs-Thymol nano-hybrid showed superior durability performance if compared to both pure PA11 and PA 11 blend realized by simply adding thymol and HNTs to polymer matrix. Furthermore, we found that HNTs and thymol combined in the nano-hydrid form exhibited an active and synergic role to achieve a major photo stabilization of PA11 biocomposite, without sacrificing its mechanical properties.

**Corresponding author: phone: +39-(0)95-7338236; fax: +39-(0)95-7338206; e-mail address: sabrinacarola.carroccio@cnr.it.*

Keywords: PA11, halloysite, thymol, nanocomposites, ball milling, photo-oxidation, UV irradiation, mechanical properties, degradation, release.

1. Introduction

Plastic materials derived from renewable resources for replacement of petroleum-based ones are gaining growing interest both in industry and in the scientific research community. Polyamide-11 (PA11) obtained from castor beans [1, 2], is a promising material as "green" alternative in a variety of applications ranging from household devices to engineering materials. At the present, PA11 finds excellent placings in metal coatings, flexible pipes for automotive and offshore applications. PA11 exhibits in fact outstanding mechanical properties (high fatigue resistance, low frictional coefficient, excellent creep resistance) and good chemical resistance. Furthermore, its potential ability in replacement traditional polymeric materials, especially where mechanical properties and flame resistance are required, could be enhanced by formulating it as nanocomposites [3,4]. From the degradation point of view, it is well known that polyamides (PAs) are not intrinsically stable in the presence of oxygen and/or humidity, especially at high temperature [5-11]. In particular, aliphatic polyamides undergo to degradation during processing and outdoor applications, involving a drastic drop in term of mechanical and physical properties [12]. Improvement in thermal stability of PA11 was observed by adding clays [13] and carbon nanotubes [14] whereas hydrolytic resistance was achieved by adding graphene [15]. Nevertheless, organic and inorganic fillers might affect in different ways the durability of nanocomposites [16- 18], especially in terms of photo and thermo-oxidative stability of polymer matrix [19, 20].

Recently, a new class of green and naturally abundant fillers for polymers, halloysite nanotubes (HNTs), is attracting great interest for the peculiar chemical composition and physical shape. They are alumosilicate sheets rolled into tiny tubes with general chemical formula $Al_2Si_2O_5(OH)_4 \times nH_2O$ [21, 22]. The length of HNTs is about 1000 nm, the internal diameter ranges in 10-15 nm, and the external diameter is about 50-80 nm. Due to the tubular shape, HNTs can be dispersed in polymer matrices without exfoliation, as required for a good dispersion of layered clays. They have been widely used as filler for polymers as reservoirs of active molecules (drugs, antimicrobials, flame retardants, essential oils, self-healing agents, anticorrosion molecules, etc…) [23-31], imparting structural and functional properties to the materials. At the same time, HNTs are used for attaining advanced mechanical and/or thermal features [20, 32, 33]. Recently, a dramatic pro-degradant effects of HNTs on the photooxidation of PLA was reported by Therias et al. [20]. When this happens, the benefits deriving from the addition of fillers into the polymer matrix are counteracted, severely preventing the application of this material for outdoor exposure.

In this paper we investigated the accelerated photo-aging of a novel PA11 hybrid composite, formulated by using HNTs as nano-containers of a light stabilizer. In view of packaging application,

thymol (2-isopropyl-5-methylphenol), a phenolic antioxidant with high relevance in free radical scavenging processes [32, 33], is tested as potential green additive for its harmlessness at low concentration.

The nano-hybrid was dispersed into the PA11 matrix using mechanical energy (high energy ball milling) at ambient temperature and in dry conditions. The molecular and structural data obtained from SEC and MALDI spectra of photo-exposed PA11 nano-hydrid composite are reported and discussed. Both thermal and mechanical properties as well as thymol release of the formulated PA11 samples were also tested and compared with referenced samples.

3. Experimental

3.1. Materials

PA11 (ρ = 1.026 g ·cm^{-3} at T = 25 °C, glass transition temperature T_g = 46°C and melting temperature T_m = 198 °C), 2-(4 hydroxyphenilazo)benzoic acid (HABA), hexafluoroisopropanol (HFIP), Halloysite nanoclay powders (CAS 1332-58-7) and thymol powders (CAS 89-83-8) were all supplied from Sigma Aldrich (Italy) and were used as received.

3.2 Preparation of HNTs/Thymol nanohybrid

3 g of Thymol were dissolved in 30 ml of distilled water at 50°C for 20 mins. 3 g of HNTs were then mixed to the Thymol solution and ultrasonic processing was performed for 10 minutes to allow HNTs sufficiently dispersed. The solution was heated at 50°C for 2 min, then vacuum (0.085 MPa) was applied to remove the air between and within the hollow tubes. The vacuum was maintained for 15 min. The solution was then taken out from the vacuum and shaken for 5 min. Vacuum was re-applied, for 15 mins, to remove the trapped air. The thymol loaded HNTs were dried in an oven for 72 h at 50°C to reach a constant weight. The content of Thymol (wt%) in the HNT-Thymol hybrid was calculated, using the TGA analysis, according to following equation:

$$\alpha_3 = w \cdot \alpha_1 + (1 - w) \cdot \alpha_2$$

where α_1 is the mass loss of Thymol at 800°C; α_2 is the mass loss of HNTs at 800°C; α_3 is the mass loss of HNTs-Thymol at 800°C °C (see Figure 1). The content of Thymol (wt%) in HNTs-Thymol hybrid was estimated to be 55.5% and the HNTs content was 44.5%.

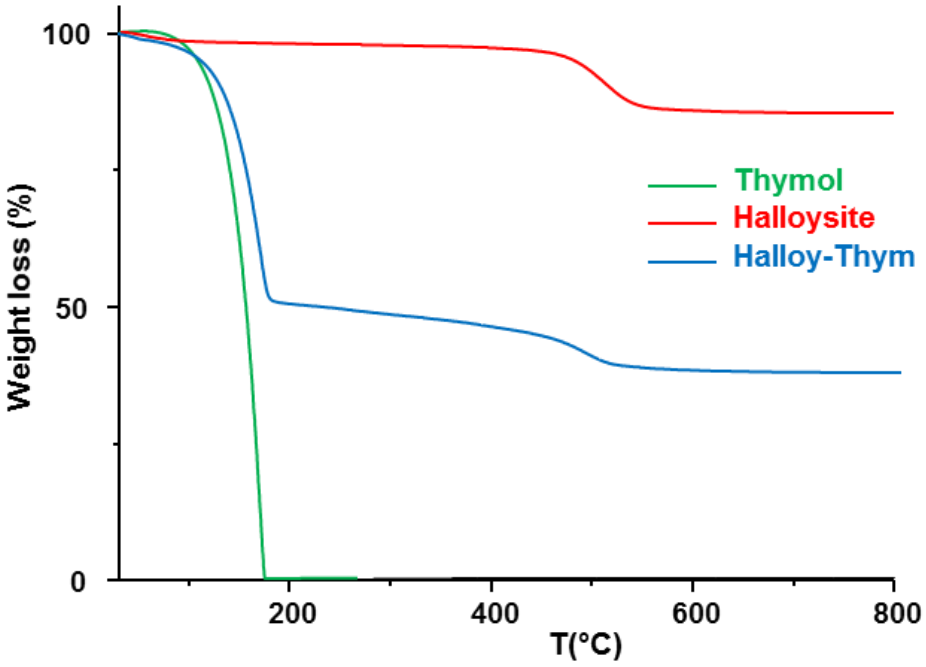

Figure 1. Weight loss, measured by TGA at 800 °C, of HNTs-Thymol nanohybrid, Thymol and HNTs

The incorporation of the HNTs-Thymol hybrid into PA11 was achieved using the High Energy Ball Milling (HEBM) technology. The powder mixture composed of PA11 and HNTs-Thymol (vacuum dried for 24h) at 10 wt% was milled at room temperature in a Retsch (Germany) centrifugal ball mill (model S 100). The milling process occurred in a cylindrical steel jar of 50 cm^3 with 5 steel balls of 10 mm of diameter. The milling time was 60 mins and the rotation speed was 580 r.p.m. Pure PA11 and PA11 with 5.55% of thymol, PA11 with 4.45% of HNTs and PA11 with 4.45% of HNTs and 5.55% of thymol blends were milled in the same experimental conditions of the composite and taken as references.

3.3 Film preparation

Polymeric films were obtained by compression molding in a Carver laboratory press between two Teflon sheets, at 200°C, followed by cooling at ambient temperature. Their thickness was ca. 150±2 µm.

3.4 Methods of analysis

The photo-oxidative degradation of PA 11, PA11 blends and composite films was carried out on a QUV PANEL apparatus at 60 °C with continued exposure to UV radiation up to 7 days, in absence

of water. At least two separate films were analyzed at each exposure time. The irradiance (0.68 W/m^2) of the UV lamps has a broad band with a maximum at 340 nm (UVA 340 lamps).

To perform Size Exclusion Chromatography (SEC) and Matrix Assisted Laser Desorption Ionization-Time of Flight Mass Spectrometry (MALDI-TOF MS) analyses, photo-oxidized films withdrawn at different degradation times, were solubilized in HFIP and filtered.

The molar mass distribution (MMD) of polymers was determined by a multi-detector SEC system using two on-line detectors: (*i*) a multi-angle light scattering (MALS); (*ii*) a differential refractometer (DRI) as concentration detector. The SEC-MALS system consists of an Alliance 2695 separation module from Waters with a serial setup Alliance-MALS-DRI. Experiments were carried out at T = 40 °C using two PLgel Mixed C columns (5 μm particle size) from Polymer Laboratories. HFIP + 0.02M Tetraethylammonium Nitrate salt was used as mobile phase. The flow rate was 0.5 mL/min and the sample concentration was ~3 mg/mL.

The MALS on-line detector uses a vertically polarized He-Ne laser (wavelength 632.8 nm) and measures simultaneously the intensity of the scattered light at 18 fixed angular locations ranging 14.0° to 166.0°. An on-line MALS detector coupled to a concentration detector allows to obtain the absolute molar mass and the radius of gyration of each fraction of eluting polymer. The calibration constant was calculated using toluene as standard, assuming a Rayleigh factor of 1.406×10^{-5} cm^{-1}. The angular normalization of the different photodiodes was performed by measuring the scattering intensity of a poly(methyl methacrylate) standard. The use of a multi-detector SEC-MALS system was described in more detail in the literature [32, 33].

MALDI-TOF mass spectra were recorded in reflector mode using a Voyager-DE STR (*Applied Biosystems*) mass spectrometer equipped with a nitrogen laser emitting at 337 nm with a 3-ns pulse width and working in positive ion mode. The accelerating voltage was 20 kV; the grid voltage and the delay time were optimized for each sample to achieve the higher molar mass values and the best resolution. The laser irradiance was maintained slightly above threshold. HABA (0.1 M in HFIP) was used as matrix. Appropriate volumes of polymer solution (5 mg/mL in HFIP) and matrix solution were mixed to obtain 2:1, 1:1, and 1:2 ratios (sample/matrix v/v). Cationizing agents (NaTFA, KTFA, LiTFA) were also used to improve the quality of spectra as well as discriminate possible structures during the peak assignment. 1 μL of each sample/matrix mixture was spotted on the MALDI sample holder and slowly dried to allow matrix crystallization. At least three separate PA11 portion were analyzed at each heating time. The resolution of the MALDI spectra reported in the text is about 9000-12000 FWHM, and the accuracy of mass determination was about 250 ppm in the mass range of 1000-3000 Da. The structural assignment of MALDI peaks in Table 2 was mainly made on the basis of empirical formulas. However, isotopic resolution helps considerably in the peak-assignment

process through the comparison of the relative intensities of isotopic peaks corresponding to oligomers of increasing molar mass. When necessary, to distinguish and separate between the contribution of isotopic peaks M + 1 and M + 2 and peaks due to isobaric structures, a deisotoping program (Data explorer ® software) was used. This program produces a theoretical spectrum for each species and subtracts from experimental spectrum the intensity calculates values of M + 1 and M + 2 isotopic peaks. The relative amount of peak at *m/z* 1293.44 was obtained as the ratio IA/IB where IA is the peak intensity of selected species and IB corresponds to the intensity of base peak appearing in the same mass range.

The thermogravimetric analyses of the films submitted to photo-degradation were performed using a thermogravimetric apparatus (TGA, TA Instruments Q500) under air atmosphere (flow rate 60 mL/min) at 10 °C/min heating rate, from 40 °C to 800 °C. Sample weights were approximately 4-6 mg. The weight loss percent and its derivate (DTG) were recorded as a function of temperature.

Stress strain curves were evaluated using a dynamometric apparatus INSTRON 4301 in tensile mode at 10 mm/min. Experiments were conducted at room temperature on PA11 and composites' films submitted to different photo-degradation times. The specimens were 10 mm wide and ≅ 150 μm thick. The initial length of the samples was 10 mm. Elastic modulus was derived from the linear part of the stress-strain curves, giving to the samples a deformation of 0.2%. Data were averaged on five samples.

The release kinetics of the thymol were performed at ambient temperature using a Spectrometer UV-2401 PC Shimadzu (Japan). The tests were performed using rectangular specimens of 4 cm^2 and same thickness (≅150 μm), placed into 25 mL of ethanol and stirred at 100 rpm in an orbital shaker (VDRL MOD. 711+, Asal S.r.l.). The release medium was withdrawn at fixed time intervals and replenished with fresh medium. The considered band was at 221 nm. Results were averaged on three replicates.

4. RESULTS and DISCUSSION

To identify degradation mechanisms, photo-products, variation in MMs and MMD involved during photo-oxidation of the materials, PA11 composite samples were analysed by using SEC and MALDI methods. Thermal and mechanical properties of photo-exposed samples were also performed to determine changes in the material behaviour.

Evaluation of Molar Masses values

Figure 2 shows the MMs values of PA11, PA11 composite containing 10 wt% of HNTs-thymol hybrid, PA11 blend filled with HNTs and Thymol in the same percentage of the nano-hybrid (5.55 wt% of Thymol and 4.45 wt% of HNTs), blend of PA11 filled with 5.55 wt% of Thymol and blend

of PA11 filled with 4.45 wt% of HNTs, all the samples collected up to 7 days of photo-degradation. From the evaluation of both Mw and Mn and polydispersity index (PI) values (Table 1) of pure PA11(Figure 2 A-B) and HNTs-PA11(Figure 2 C-D) samples, it is evident a linear decrease with the exposure time, confirming that chain scissions occur during the photo oxidation process. These results agree with those reported in literature for the analogous PA 6, underwent to similar photo aging procedure [9]. As reported in literature, the addition of nanoparticles negatively influences the durability of the nanocomposite materials under UV-light exposure. The studies that have been published show that the impact depends on the functionality of the nanoparticles [16-18].

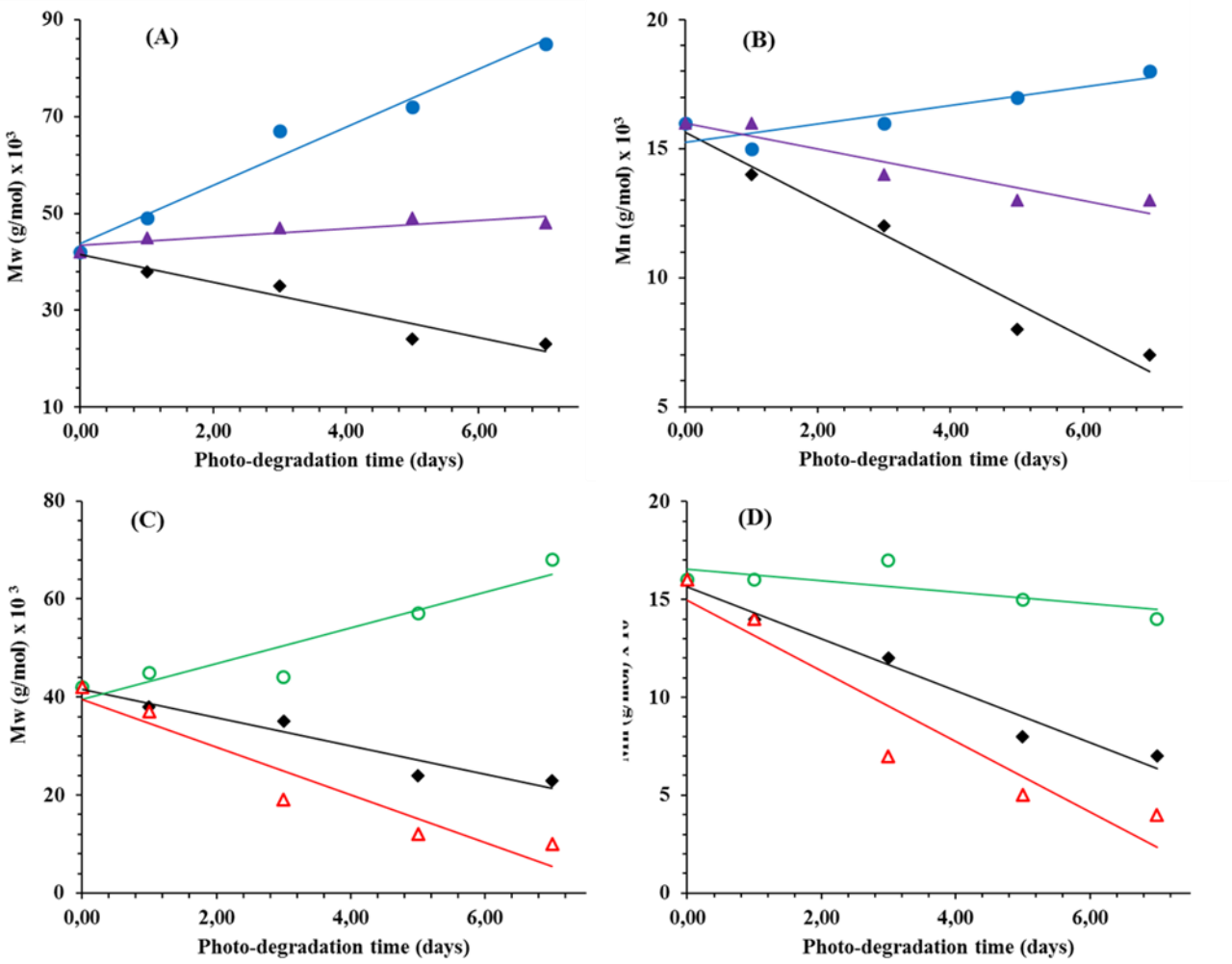

Figure 2. (A-C) Mw (g/mol) and (B-D) Mn (g/mol) as function of photo-degradation time (days) for PA11 (♦), composite of PA11 filled with 10 wt% of HNTs-Thymol nano-hybrid (●), blend using HNTs and Thymol in the same percentage of the nano-hybrid (5.55 wt% of Thymol and 4.45 wt% of HNTs) (▲), blend of PA11 filled with 5.55 wt% of Thymol (o) and blend of PA11 filled with 4.45 wt% of HNTs (Δ)

If compared with the pristine PA11 sample, SEC data collected for photo-exposed PA11/HNTs formulations, evidence a faster depletion of MMs values. This dramatic pro-degradant effect was registered also for PLA/HNTs and PA6/HNTs nanocomposites during oxidative aging [19, J. APPL.

POLYM. SCI. 2017, DOI: 10.1002/APP.45360]. The acceleration of degradative processes was ascribed to the presence of chromophoric groups and/or traces of iron into the HNTs .

As displayed in Figure 2C, the addition of thymol to the PA11 matrix reveals an opposite trend if compared with the previous samples. In fact, both MMs values registered in the whole investigated time intervals (Figures 2B-D) increase. Similarly, the PA11 filled with the nano-hybrid HNTs-Thymol (Figure 2 A-B) shows an increase of MMs with the photo-exposure time. Differently, quite constant values of Mw is experienced from the PA11 filled with HNTs and Thymol, whereas Mn slightly decreases Figure 2 (A-B).

Table 1. Polydispersity Index values of PA11 composite samples obtained by SEC-MALS data in HFIP

	Polydispersity Index (M_w/M_n) values				
Time days	PA 11	PA11 / Thymol	PA11 / Halloysite	PA11 / HNTs-Thym blend	PA11 / HNTs-Thym nanocomposite
T0	2.65	2.60	2.55	2.56	2.83
1	2.67	2.98	2.78	2.91	3.37
3	2.97	2.60	2.90	3.44	5.27
5	3.04	3.69	2.73	3.77	3.62
7	2.93	4,99	3.03	3.78	4.65

The relevant increment of Mw values of photo-exposed PA11/thymol samples clearly indicates the occurrence of crosslinking phenomena during photo-oxidation. Indeed, under oxidant condition, thymol molecules might lead to the formation of phenoxy-radicals species able to induce crosslinking reactions [35]. In particular, these reactions are predominant in the PA11/nanohybrid (Fig. 2, Table 1) whereas appear to be less pronounced in the other samples.

2. MALDI-TOF MS analysis

As well stated in the literature, MALDI MS analysis is able to explore the finest structural details in polymer degradation. In fact, whatever the cause, the deterioration mainly yields degradation products bearing characteristic end groups, which can be revealed and differentiated by MS, being indicative of specific degradation pathways [36, 37]. The degradation products produced during photo-oxidation of polyamides 6 and 66 were determined by MALDI analysis, allowed drawing a detailed map of the

photo-oxidation mechanisms [9,10]. In fact, the identification of the end groups attached to the oligomers produced is of remarkable importance, since it may reveal the particular mechanism that has been active in the degradation processes. Besides the well-known H-abstraction and subsequent formation of a hydroperoxide intermediates [38, 39], two other major processes appeared to be operating: chain-cleavage reactions Norrish type I and 2. Remarkably, the relative amount of the photo-oxidation products, representative of the three oxidation mechanisms, showed that both Norrish I and II appeared after an induction period, whereas H-abstraction is active immediately [9,10]. **Table 2** lists the oligomer structures assigned to the mass ions appearing in the MALDI spectra of pristine and photo-oxidized PA11, PA11 HNTs-Thymol blend and PA11 nano-hybrid HNTs-Thymol samples. It also specifies which photo-oxidation mechanisms is responsible for the formation of each new oligomers, adopting a special code: αH for hydroperoxides; N1 for Norrish I, NII for Norrish II and E for end groups bearing to the unexposed PA11 sample.

The MALDI spectrum of pure PA11 sample is presented in previous paper [8], therefore in Figure 3 is showed an expanded portion from 1304 to 1346 *m/z*, whereas in the supporting information the entire spectrum is reported (Fig. 1S).

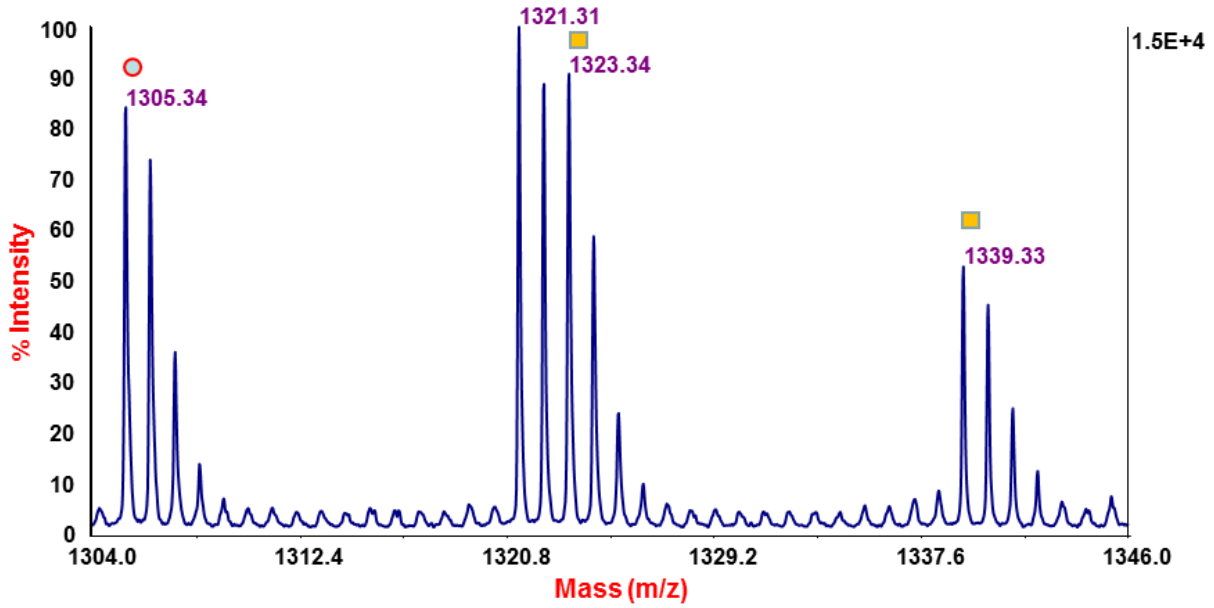

Figure 3. Expanded view of the 1294-1346 *m/z* region of MALDI-TOF Mass spectrum of PA11 recorded in positive reflectron mode by using HABA matrix.

The two abundant mass peaks series in Figure 3 are assigned to sodiated and potassiated ions of cyclic PA 11 chains (*m/z* 1305.34, 1321.31). The peaks with the square symbols are due to sodiated and potassiated ions of linear oligomers terminated with carboxyl at one end and amino groups at the other end (COOH/NH_2, *m/z* 1323.34). As expected from the theory, the intensity of the peaks

corresponding to cyclic oligomers (*m/z* 1305.34+183.16) decreases sensibly at higher masses [40]. Therefore, the original PA11 sample was mainly constituted of linear chains terminated with NH_2/COOH end groups (Fig. 1S).

MALDI data collected for all photo-exposed samples (PA11, PA11/ thymol, PA11/HNTs, PA11 HNT and thymol blend, PA11 HNT Thymol nanohybrid) evidenced the presence of the same characteristic species, belonging to the aforementioned (αH-abstraction, Norrish 1 and 2) photo-oxidation mechanisms. Nevertheless, their corresponding signals appear at different irradiation times, depending on the filler and/ or formulation used. MALDI spectra of Virgin PA11 samples, showed photo-degradation products after 3 exposure days whereas in PA11/HNTs the photo-products are revealed after 1 day of exposure (Figs. 2S). Similar results have been showed for PE and PP nanocomposites: the rates of oxidation were modified whereas photo-oxidation products remained the same [16].

From the inspection of MALDI spectra of photo-exposed PA11 filled with thymol, it is evident the appearance of the specific degradation peaks after 7 days of exposure. If compared with unfilled sample, we can note that a stabilization is accomplished by the presence of thymol molecules (Figs 2S).

Table 2. Oligomer structures assigned to the mass ions appearing in the MALDI spectra of photo-oxidized pure PA11, PA11 HNTs-Thymol blend and PA11 nano-hybrid HNTs-Thymol samples. a) Terminal groups originated by specific photo-oxidation processes: αH hydroperoxides; N1 Norrish I; NII Norrish II; E end groups of the unexposed PA11.

Photo-degradation mechanisms [a)]	**Structures**	**MNa^+**	**MK^+**
E	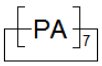	**1305.34**	**1321.31**
N1	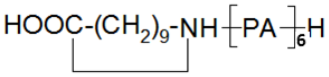	**1309.45**	,
E-αH	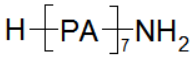	**1322.50**	**1338.40**

E- αH	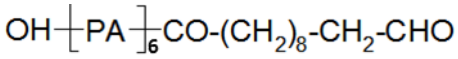	**1322.50**	**1338.40**
E	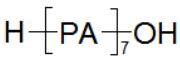	**1323.34**	**1339,33**
N1-N1	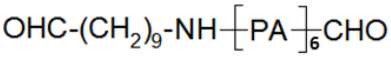	**1321.31**	**1337.51**
E- αH	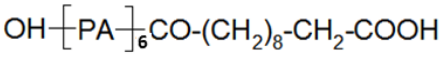	**1338.40**	**1354.50**
N1-E	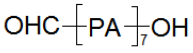	**1351,53**	**1367.51**
N1- αH	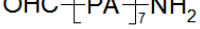	**1350,53**	/
N1-N1	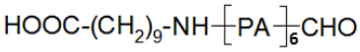	**1337.51**	**1353.50**
αH-N2	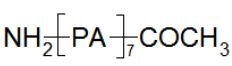	**1364.50**	/
E-N2	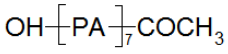	**1365.51**	/
E-N2	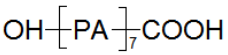	**1367.51**	/
N1-N1	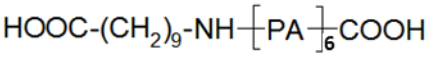	**1353.49**	/
N1-E	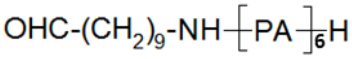	**1293.44**	**1309.45**

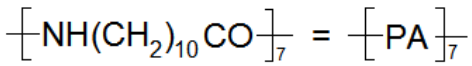

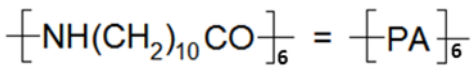

Rather unusual, the spectra collected for PA11 filled with nano-hybrid HNTs-Thymol and PA11 HNTs-thymol blend formulated with the same percentage of the nano-hybrid (5.55 wt% of Thymol and 4.45 wt% of HNTs, revealed significant differences. In **Figure 4 A-B** are reported the MALDI spectra of PA11 nano-hybrid HNTs/thymol photo-exposed for (A) 7 days and PA11 HNTs-thymol blend for (B) 3 days. The spectrum in Fig. 4A appears quite similar to the pristine PA11 sample (Fig. 3) whereas several new peaks, assigned to photo-products (Table 2), are revealed in the PA11 Thymol-HNT blend photo-exposed for 3 days (Fig. 4 B). In the spectra (Fig. 4A-B), the peaks at *m/z* 1323.34 belong to $COOH/NH_2$ oligomers, whereas, the prominent peak at *m/z* 1322.50 after deisotoping procedure (see experimental part), can be reasonable assigned to photo products having $CONH_2/NH_2$ as well as the isobaric structure bearing OH/CHO as terminal groups. Both of them, are obtained from αH abstraction mechanisms. As reported in the literature, at $\lambda > 340$ nm chromophore defects, and impurities initiate αH-abstraction followed by hydro-peroxidation. Thermal and photochemical decomposition of ROOH occurs through the homolysis of the peroxidic bond. However, it has been shown that ROOH did not initiate any new oxidative propagation process. This is consistent with a preferential recombination of the radicals formed (especially the very reactive OH radicals), leading to imide groups [38, 39, 41]. In the spectrum of PA11 nano-hybrid HNTs-thymol photo-exposed for 7 days (Fig. 4A), a very low intensity peak corresponding to imide terminal groups (1322,50 m/z) is evident after deisotoping procedure. Furthermore, species at 1339,40 m/z is unequivocally assigned to potassiated imide terminal groups. This suggests the material is experiencing the early stage of degradation process. However, the peaks at m/z 1293.44, 1353,49, 1364,51, 1367,51, 1337,51 and 1350,53 revealed in the Fig. 4B, are connected to degradation products coming also from NORRISH I and NORRISH II photo-cleavage reaction (Table 2). For aliphatic polyamides, such kind of processes [9, 10], indicate a significant degradation level of material. After 7 days of photo-exposure, film appeared extremely fragile. MALDI data collected from this sample show signals in the lower mass range, overlapping matrix cluster peaks, and thus difficult to assess.

As visible from Fig. 2 A-B, SEC data acquired for the latter sample do not exhibit sensible change in MMs values. This fact is most likely due to a balance effect in terms of MMs during photo-oxidation of PA11 Thymol-HNTs blend. In fact, SEC data of PA11/HNTs showed a sensible depletion of MMs

values. However, if the PA11 is filled with only the thymol, it works as antioxidant inducing at the same time a significant increment of MMs values. Reasonably, if the two fillers (HNTs and thymol) are added together, chain scissions, stabilization and crosslinking reactions take place in concomitance, producing a level of MMs during exposure. In agreement with the MALDI spectrum reported in Figure 4A, where any N1 and N2 photo-degradation products peaks appearing, the relevant increment of MMs values for nano-hybrid HNTs/thymol (Fig. 2 A-B) indicated as main reaction the occurrence of branching and/or crosslinking.

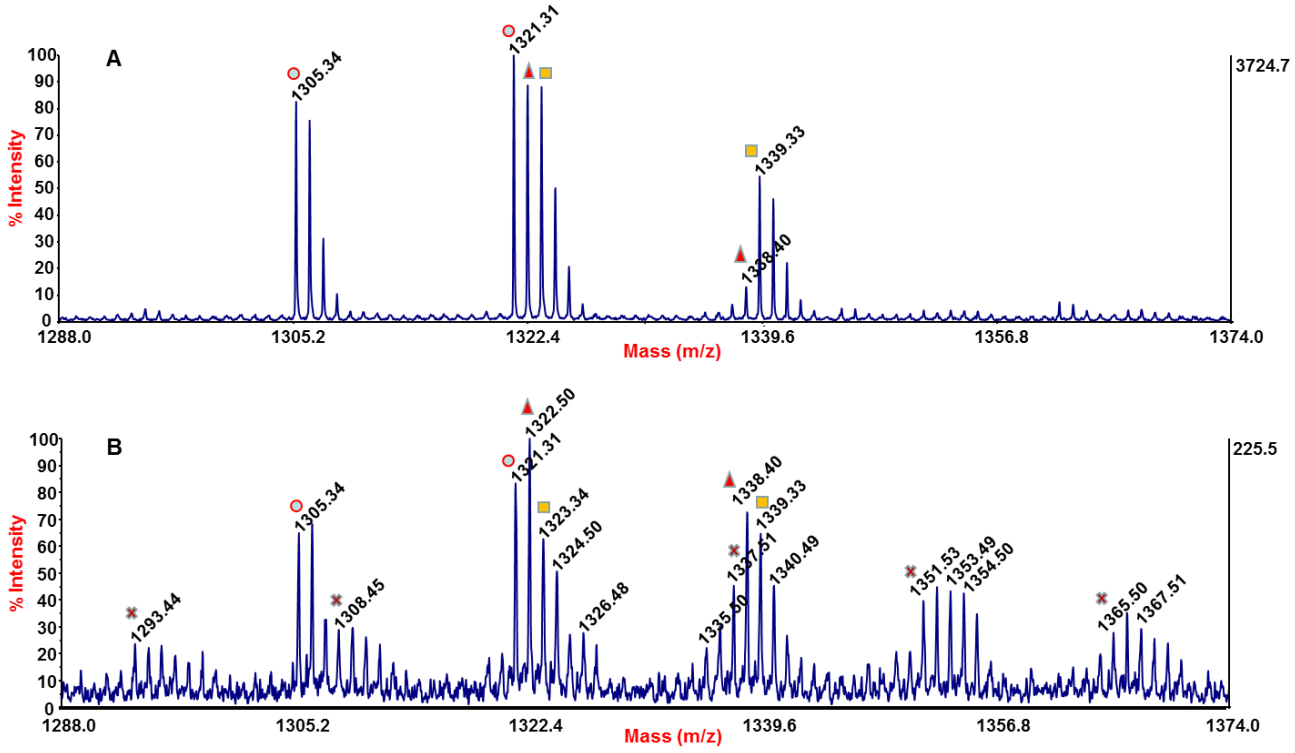

Figure 4. MALDI-TOF Mass spectra in the mass range 1288-1374 *m/z* of PA11 nano-hybrid HNTs-Thymol photo-exposed for (A) 7 days and PA11 blend of HNTs and Thymol in the same percentage of the nano-hybrid (5.55 wt% of Thymol and 4.45 wt% of HNTs) for (B) 3 days.

In figure 5 was reported the relative amount of a characteristic peak (m/z 1293,44) deriving from Norrish 1 photo-process, as a function of time exposure.

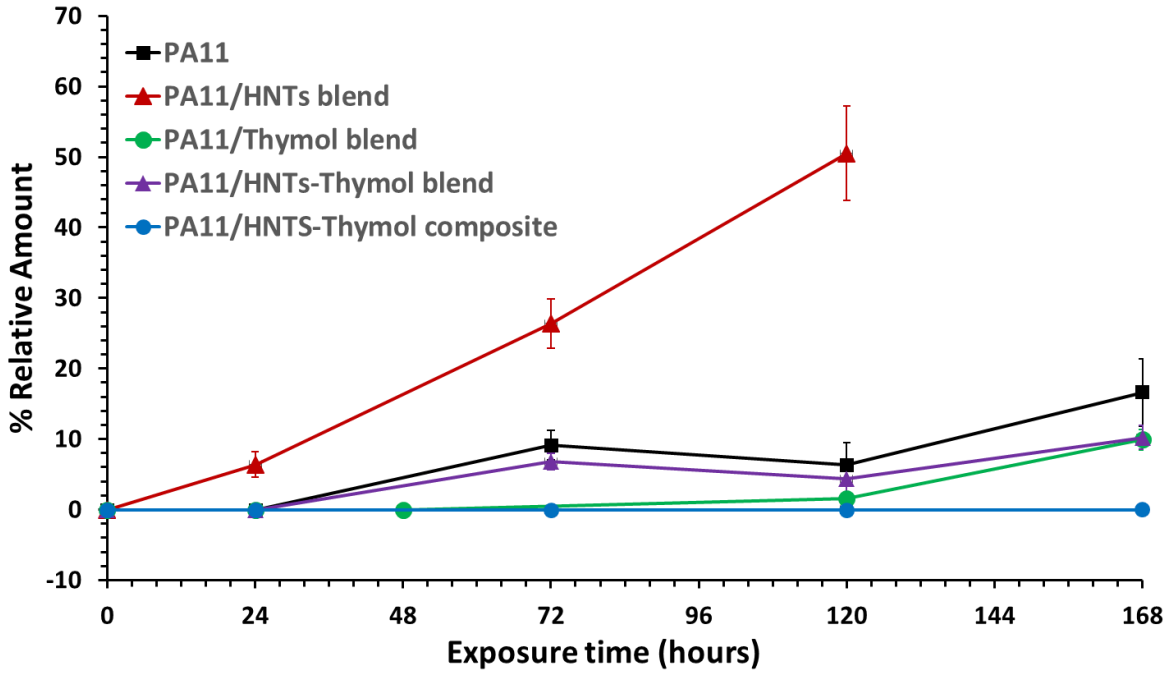

Figure 5. % relative amount of a characteristic peak (m/z 1293,44) deriving from Norrish 1 photo-process as a function of time exposure.

The pristine PA11 and PA11/HNTs-Thymol blend samples showed photo-degradation product after 3 exposure days, whereas PA11/HNTs displayed the same degradation peaks after 1 day of exposure (Fig 2s). In the case of PA11/Thymol blend the peak corresponding to the photo products is visible after 7 days of UV exposure (Fig. 5 and 2S), indicating that thymol is able to extend in time the stability of PA11 against photo-oxidative degradation. Particularly, the stabilization of thymol is significantly prolonged in the PA11/Thymol-HNTs nanohybrid formulation, although the presence of HNTs into the the blend.

Experimental data suggest as the peculiar position of thymol in such formulation plays a key role, accomplishing a superior anti-oxidant ability if compared with the all PA11 samples investigated. Obviously, also in the nanohybrid formulation, part of the thymol molecules are adsorbed onto the external wall of HNTs, thus their photo protection effect towards the PA11 sample could not be different from the other formulation. Additionally, during the aging, as the majority of low molecular weight additives, thymol can diffuse out of the polymer, when it may be lost by volatilization. Consequently, thymol concentration in a PA11 matrix faster decreases in any formulations. However, the results obtained from PA11/Thymol-HNTs in term of oxidative stability, suggest that a slower release of thymol molecules is accomplished by the cage effect, of HNTs nanocontainers. This implies a time-prolonged permanence of stabilizer into the polymer during photo-oxidation, that contributes in a sensible way on material durability considering that HNTs is part of the formulation.

To verify this hypothesis, we performed measurements of controlled thymol release in ethanol from the sample PA11/HNTs-Thymol composite, containing 5.55 wt% of thymol, and the sample where thymol is simply blended to the polymer at the same concentration (5.55 wt%) of hybrid. Data are reported in Figure **6**. It is evident a fast release of thymol in the sample where it is simply blended with PA11, that reaches the 100% of release already at 48h. The nano-composite containing the thymol dispersed with HNTs shows a slow release and after one month, the percentage of molecule released is around 68%.

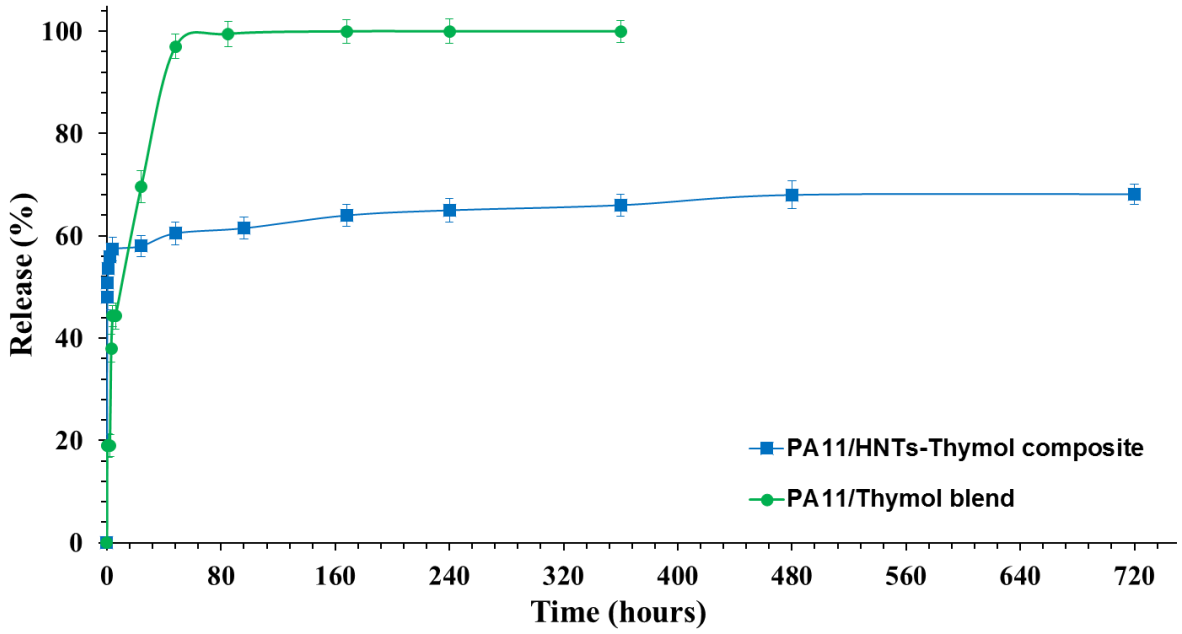

Figure 6: Release (%) of thymol in ethanol from PA11/HNTs-Thymol composite (5.55% of thymol) and PA11/thymol (5.55%) blend

Mechanical and Thermal properties

Figure 7 reports the elastic modulus, E (MPa), as function of photo-degradation time (days) for pure PA11 and PA11 HNTs-Thymol composite. The unaged samples show a little difference in the elastic modulus. The sample filled with the nano-hybrid shows E (MPa) slightly higher than that of unfilled PA11. This is due to a reinforcing effect of the inorganic phase (4.45 wt% of HNTs) into the polymer matrix. One day of photo-degradation does not significantly modify the value of such mechanical parameter, in fact, it remains quite the same for both samples and similar to that of unaged materials. From 3 to 7 days of photo-degradation the unfilled sample shows a drop in the modulus that decays from 433 MPa (unaged) to 250 MPa. This is in accordance with SEC analysis, where a decrease of MMs values are observed in function of irradiation time. Opposite trend is shown by the composite filled with 10 wt% of HNTs-Thymol, where the modulus increases with the photo-degradation time.

In accordance with the increasing of MMs, evaluated by SEC, the improvement of the elastic modulus can be associated with this phenomenon. Furthermore, the presence of the HNTs could also help the sample to retain a good mechanical consistence even after 7 days of photo-degradation treatment. Elongation at break (%) and tensile strength (MPa) data follow the same trend of the elastic modulus (see supporting information).

The results of TGA characterization for pure PA11, PA11 HNTs-Thymol composite and blend, are summarized in Table 1S. The temperature at the maximum derivative of weight loss (TD) of nanohybrid formulation increases of 24 °C if compared with the pure PA11 sample, while an increase of 10 °C was registered for the blend sample. These data, suggest that a superior stabilization effect against thermo-oxidation process in air is acted by nanohydrid formulation.

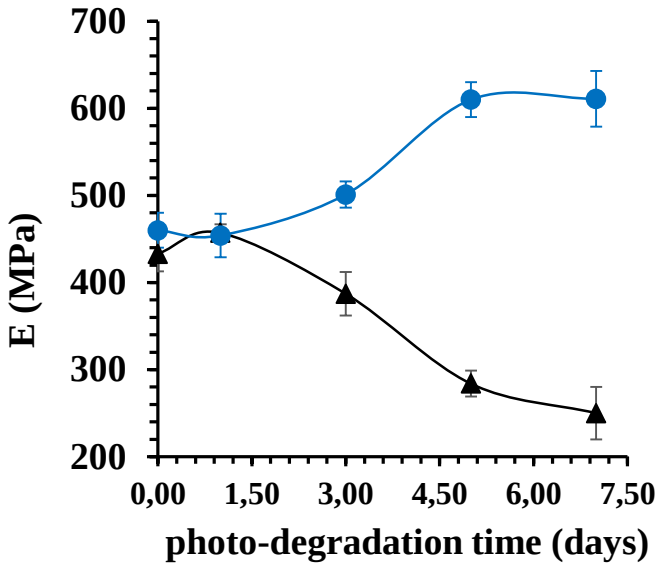

Figure 7. Elastic modulus, E (MPa), as function of photo-degradation time (1-3-5-7 days), of pure PA 11 (▲) and PA11 nano-hybrid HNTs-Thymol (●).

4. CONCLUDING REMARKS

In this work the formulation of a biocomposite based on PA11 and a nano-hybrid HNTs-Thymol by using ball-milling as compounding procedure is reported. Thymol, entrapped into the lumen of halloysite nanotubes, was chosen as green antioxidant and its ability in protecting polymer matrix from UV irradiation in presence of air was tested. Data collected by using SEC and MALDI MS as well as by thermal and mechanical analyses, evidence peculiar features depending on fillers and/or PA11formulations used. If compared with all samplestested, the molecular and structural data revealed a sensible contribution of HNTs/thymol nano-hybrid in stabilizing the polymer matrix. We suppose that a synergic effects between them was accomplished: while thymol avoids the acceleration

of oxidative reactions deriving from HNTs fillers, the latters, working as nano-containers, perform a slower release of thymol molecules into the PA11 bulk during photo-exposure. This effect significantly contributes to durability of polymer material although the presence of a pro-degradant filler. At the same time, the a significant improvement of the thermal properties and elastic modulus during UV irradiation is also experienced by the aliphatic polyamide matrix thank to the HNTs fillers.

Acknowledgment. Partial financial support from Ministry of University and Research in Italy is gratefully acknowledged.

References

[1] D.S. Ogunniyi, Castor oil: A vital industrial raw material, Bioresour. Technol. 97 (2006) 1086 1091. doi:10.1016/j.biortech.2005.03.028.

[2] W. Lu, J.E. Ness, W. Xie, X. Zhang, F. Liu, J. Cai, J. Minshull, R.A. Gross, Biosynthesis of monomers for plastics from renewable oils, in: ACS Symp. Ser., 2012: pp. 77–90. doi:10.1021/bk-2012-1105.ch006.

[3] A. Hao, I. Wong, H. Wu, B. Lisco, B. Ong, A. Sallean, S. Butler, M. Londa, J.H. Koo, Mechanical, thermal, and flame-retardant performance of polyamide 11–halloysite nanotube nanocomposites, J. Mater. Sci. 50 (2015) 157–167. doi:10.1007/s10853-014-8575-7.

[4] L. Ferry, R. Sonnier, J.M. Lopez-Cuesta, S. Petigny, C. Bert, Thermal degradation and flammability of polyamide 11 filled with nanoboehmite, J. Therm. Anal. Calorim. 129 (2017) 1029–1037. doi:10.1007/s10973-017-6244-1.

[5] E. Richaud, O. Okamba Diogo, B. Fayolle, J. Verdu, J. Guilment, F. Fernagut, Review: Auto-oxidation of aliphatic polyamides, Polym. Degrad. Stab. 98 (2013) 1929–1939. doi:10.1016/j.polymdegradstab.2013.04.012.

[6] B.J. Holland, J.N. Hay, Thermal degradation of nylon polymers, Polym. Int. 49 (2000) 943–948. doi:10.1002/1097-0126(200009)49:9<943::AID-PI400>3.0.CO;2-5.

[7] M.J. Oliveira, G. Botelho, Degradation of polyamide 11 in rotational moulding, Polym. Degrad. Stab. 93 (2008) 139–146. doi:10.1016/j.polymdegradstab.2007.10.004.

[8] G. Filippone, S.C. Carroccio, R. Mendichi, L. Gioiella, N.T. Dintcheva, C. Gambarotti, Time-resolved rheology as a tool to monitor the progress of polymer degradation in the melt state - Part I: Thermal and thermo-oxidative degradation of polyamide 11, Polym. (United Kingdom). 72 (2015) 134–141. doi:10.1016/j.polymer.2015.06.059.

[9] S. Carroccio, C. Puglisi, G. Montaudo, New vistas in the photo-oxidation of nylon 6, Macromolecules. 36 (2003) 7499–7507. doi:10.1021/ma0344137.

[10] S. Carroccio, C. Puglisi, G. Montaudo, MALDI investigation of the photooxidation of nylon-66, Macromolecules. 37 (2004) 6037–6049. doi:10.1021/ma049521n.

[11] S. Carroccio, C. Puglisi, G. Scaltro, T. Ferreri, G. Montaudo, Matrix-assisted laser desorption/ionization time-of-flight investigation of Nylon 6 and Nylon 66 thermo-oxidation products, Eur. J. Mass Spectrom. 13 (2007) 397–408. doi:10.1255/ejms.899.

[12] Allen, N. S., McKellar, J. F. The photochemistry of commercial polyamides. *J. Polym. Sci. Macromol. Rev.* **13** (1978) 241–281.

[13] Y. Li, G. Hu, B. He, Thermal stability, crystallization and mechanical properties of nylon11 / montmorillonite nanocomposites, E-Polymers. 60 (2011) 1–11.

[14] J. Bai, S. Yuan, F. Shen, B. Zhang, C.K. Chua, K. Zhou, J. Wei, Toughening of polyamide 11 with carbon nanotubes for additive manufacturing, Virtual and Physical Prototyping 12 (3), 235-240

[15] S.J.A. Hocker, N.V. Hudson-Smith, P.T. Smith, C.H. Komatsu, L.R. Dickinson, H.C. Schniepp, D.E. Kranbuehl, Graphene oxide reduces the hydrolytic degradation in polyamide-11, Polymer 126 (22) (2017) 248-258

[16] A. P. Kumar, D. Depan, N. S. Tomer, R. P. Singha, Nanoscale particles for polymer degradation and stabilization—Trends and future perspectives, Progress in Polymer Science 34 (2009) 479–515

[17] M. Nechifoar, D. Photochemical Behavior of Multicomponent Polymeric-based Materials. Advanced Structured Materials 26, 21-65 D. Rosu and Visakh P. M. (eds.) (2016)

[18] P.-O. Bussière, J. Peyroux, Geneviève Chadeyron, Sandrine Therias, Influence of functional nanoparticles on the photostability of polymer materials: Recent progress and further applications, Polymer Degradation and Stability 98(12), pp. 2411-2418

[19] G. Filippone, S.C. Carroccio, G. Curcuruto, E. Passaglia, C. Gambarotti, N. Dintcheva, Time-resolved rheology as a tool to monitor the progress of polymer degradation in the melt state - Part II: Thermal and thermo-oxidative degradation of polyamide 11, Polym. 73 (2015) 102–110.

[20] S. Therias , M. Murariu, P. Dubois, Bionanocomposites based on PLA and halloysite nanotubes: From key properties to photooxidative degradation, Polymer Degradation and Stability 145 (2017) 60-69.

[21] Gorrasi G, Milone C, Piperopoulos E, Lanza M, Sorrentino A (2013) Hybrid clay mineral-carbon nanotube-PLA nanocomposite films. Preparation and photodegradation effect on their mechanical, thermal and electrical properties, Applied Clay Science 71: 49-54

[21] P. Yuan, D. Tan, F. Annabi-Bergaya, Properties and applications of halloysite nanotubes: Recent research advances and future prospects, Appl. Clay Sci. 112–113 (2015) 75–93. doi:10.1016/j.clay.2015.05.001.

[22] Y. Lvov, E. Abdullayev, Functional polymer-clay nanotube composites with sustained release of chemical agents, Prog. Polym. Sci. 38 (2013) 1690–1719. doi:10.1016/j.progpolymsci.2013.05.009.

[24] E. Abdullayev, Y. Lvov, Halloysite Clay Nanotubes for Controlled Release of Protective Agents, J. Nanosci. Nanotechnol. 11 (2011) 10007-10026 doi:10.1166/jnn.2011.5724 10007

[26] G. Gorrasi, L. Vertuccio, Evaluation of zein/halloysite nano-containers as reservoirs of active molecules for packaging applications: Preparation and analysis of physical properties, J. Cereal Sci. 70 (2016) 66–71. doi:10.1016/j.jcs.2016.05.008.

[27] G. Gorrasi, Dispersion of halloysite loaded with natural antimicrobials into pectins: Characterization and controlled release analysis, Carbohydr. Polym. 127 (2015) 47–53. doi:10.1016/j.carbpol.2015.03.050.

[28] N.G. Veerabadran, R.R. Price, Y.M. Lvov, Clay Nanotubes for Encapsulation and Sustained Release of Drugs, Nano. 2 (2007) 115–120. doi:10.1142/S1793292007000441.

[29] P. Scarfato, E. Avallone, L. Incarnato, L. Di Maio, Development and evaluation of halloysite nanotube-based carrier for biocide activity in construction materials protection, Appl. Clay Sci. 132-133 (2016) 336-342. doi: 10.1016/j.clay.2016.06.027

[30] M. Liu, L. Dai, H. Shi, S. Xiong, C. Zhou, In vitro evaluation of alginate/halloysite nanotube composite scaffolds for tissue engineering, Mater. Sci. Eng. C. 49 (2015) 700–712. doi:10.1016/j.msec.2015.01.037.

[31] B. Guo, Q. Zou. Y.Lei,; M. Du,; M. Liu,; D. Jia, Crystallization behavior of polyamide 6/halloysite nanotubes nanocomposites. Thermochim. Acta 484 (2009) 48–56.

[32] C. Turek, F.C. Stintzing, Stability of Essential Oils: A Review, ComprehensiveReviews in Food Science and Food Safety, (2013) 12.

[33] R. Mendichi, A. G. Schieroni, Current Trends in Polymer Science, Vol. 6: Use of a multi-detector size exclusion chromatography system for the characterization of complex polymers. Trivandrum, India: Pandalai, (2001) 17-32.

[34] P.J. Wyatt, Light scattering and the absolute characterization of macromolecules, Anal. Chim. Acta. 272 (1993) 1–40. doi:10.1016/0003-2670(93)80373-S.

[35] T. Günay, Y. Çimen, R.B. Karabacak, H. Türk, Oxidation of Thymol and Carvacrol to Thymoquinone with KHSO5Catalyzed by Iron Phthalocyanine Tetrasulfonate in a Methanol–Water Mixture, Catal. Letters. 146 (2016) 2306–2312. doi:10.1007/s10562-016-1850-2.

[36] N.S. Allen, J.F. McKellar, The photochemistry of commercial polyamides, J. Polym. Sci. Macromol.13 (1978) 241–281. doi:10.1002/pol.1978.230130105.

[37] G. Montaudo, F. Samperi, M.S. Montaudo, S. C. Carroccio, C. Puglisi Eur. J. Mass Spectrom. 11, 1–14 (2005) doi: 10.1255/ejms.718

[38] A. Roger, J. Lemaire, D. Sallet, Photochemistry of Aliphatic Polyamides. 4. Mechanisms of Photooxidation of Polyamides 6, 11, and 12 at Long Wavelengths, Macromolecules. 19 (1986) 579–584. doi:10.1021/ma00157a015.

[39] J. Lemaire, J.L. Gardette, A. Rivaton, A. Roger, Dual photo-chemistries in aliphatic polyamides, bisphenol A polycarbonate and aromatic polyurethanes-A short review, Polym. Degrad. Stab. 15 (1986) 1–13. doi:10.1016/0141-3910(86)90002-9.

[40] G. Montaudo, S. Carroccio, F. Samperi, C. Puglisi, Recent Advances in MALDI Mass Spectrometry of Polymers, Macromol. Symp. 218 (2004) 101–112. doi:10.1002/masy.200451411.

[41] G.R. Coates, L. Xiao, M.G. Prammer, N.M.R. Logging, Principles and Applications, 1999.

1

2

3

4

5

6

7

8